Kinematics design and human motion transfer for a humanoid service robot arm

Chioniso Dube[1], *Jonathan Tapson*[2]

[1] Mobile Intelligent Autonomous Systems
Council for Scientific and Industrial Research, South Africa
cdube@csir.co.za

[2] Department of Electrical Engineering
University of Cape Town
jonathan.tapson@uct.ac.za

Abstract

This paper focuses firstly, on the kinematics structure required for a humanoid service robot arm and secondly, on transferring human motion obtained from visual motion capture to the humanoid arm. The kinematics structure of a ten Degree of Freedom (DOF) humanoid arm which has a two DOF shoulder girdle and has a four DOF glenohumeral joint is presented. A method of obtaining the sternum position, which forms the movement reference frame for the ten DOF arm, is formulated from human motion capture data. The method is based on clavicle and spine workspaces. Results show that the sternum formulation corresponds well to the actual sternum position.

1. Introduction

Humanoid robot arms have the potential for use as service or care robots in human environments such as homes, hospitals, and offices. Human environments are ergonomically designed for the human structure and range of motion. It follows that a robot arm working in such an environment should have a structure and range of motion similar to that of a human.

This paper focuses on the kinematic design of a humanoid robot arm for human environments and the transferring of human motion to the humanoid arm via visual motion capture. An African dance is chosen as a case study in human motion since dance contains many movement elements which are required for various human tasks.

Firstly, the structure and movements of the human arm are investigated, and the importance of the shoulder girdle to human arm movements and workspace is highlighted (Section 2). This is followed by a comparison of current humanoid arm designs to the human arm (Section 3). Two limitations of humanoid robots that constrain their performance when compared to human arms are the lack of a humanoid shoulder girdle, and the singularity found at the humanoid glenohumeral joint (Section 3). To address these limitations the kinematics design for a ten Degree Of Freedom (DOF) humanoid arm is presented(Section 4).

An overview of the motion capture process used to capture the human dance is then given (Section 5). Next, the inverse kinematics method used to transfer human motion to the robot arm is described (Section 7). In order to attain the reference frame for the shoulder girdle DOFs a method of extracting sternum position information from the motion capture data is formulated. Finally the formulation is compared against a test data set in order to verify the formulation (Section 6).

2. The human arm

The human arm forms the basis for humanoid arm designs. According to the movement sciences of kinesiology and biomechanics, the human arm, along with the shoulder girdle form part of the human upper limb as shown in Figure 1. Any dance movement of a human is made up of combinations of basic movements or DOFs of the human joints.

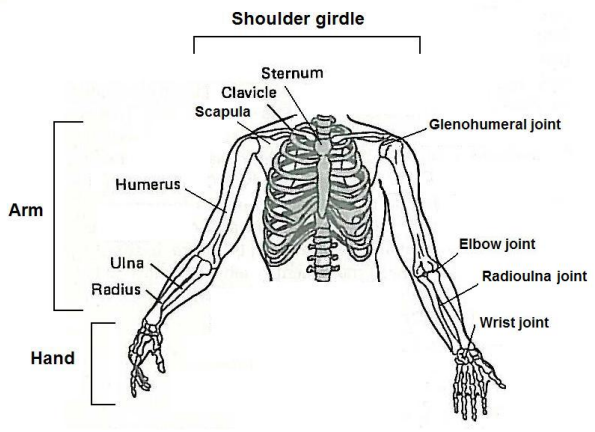

Figure 1: Human upper limb (shoulder girdle, arm and hand), showing bones and joints of the arm and shoulder girdle [1]

2.1. Human arm movements

The human arm has four joints and seven DOFs as shown in Figures 2, 3 and 4. At the glenohumeral joint are three DOFs; abduction/adduction, flexion/extension and inward/outward rotation. At the elbow joint is one DOF; elbow flexion/extension. At the radioulna is another DOF; pronation/supination. At the wrist are two DOFs; flexion/extension and abduction/adduction. [1] [2]

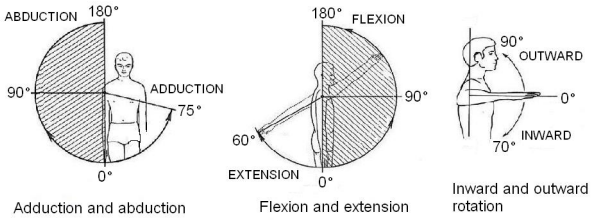

Figure 2: Human glenohumeral joint movements [1]

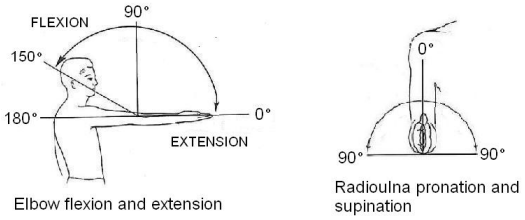

Figure 3: Human elbow and radioulna joint movements [1]

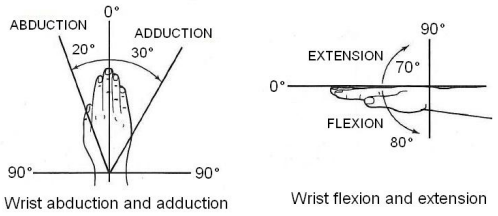

Figure 4: Human wrist joint movements [1]

2.2. Shoulder girdle effects on human arm movements

Although the human arm only has seven DOFs, the overall movements of the arm are affected by the movements of the shoulder girdle. For instance, the shoulder girdle changes the position and orientation of the centre of rotation of the glenohumeral joint thus increasing the arm workspace as well as allowing the arm to avoid collisions with the body. According to Lenacic et al, the shoulder girdle increases the human arm workspace by 50% [3]. The movements of the shoulder girdle that affect the centre of rotation of the glenohumeral joint are elevation/depression, upward tilt and protraction/retraction as shown in Figure 5 [1] [2] .

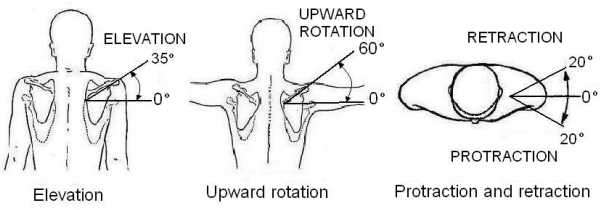

Figure 5: Human shoulder girdle movements [1]

3. Humanoid arms

Most humanoid arms, like the human arm itself have the requisite seven DOFs. There are two types of humanoid arm structure found; parallel and serial structured arms. Parallel structured arms generally have a smaller workspace than serial arms, limiting the use of parallel arms in a human environment. Serial arms, in contrast, generally have larger workspaces and are the more commonly found type of humanoid arm.

Asimo [4], HRP-2 [5], HUBO [6], and AMAR [7], are some examples of humanoid robots with serial structured arms. Figure 6 shows the structure of a typical seven DOF serial humanoid arm along with its Denavit-Hartenburg parameters. The Denavit-Hartenburg formulation is detailed in [8].

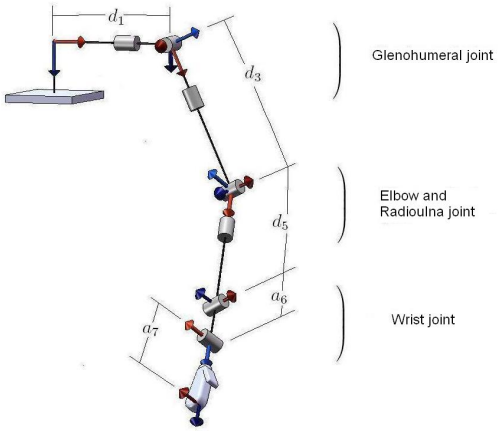

Figure 6: Kinematic structure and Denavit-Hartenberg parameters (Link length a and joint offset d) for a 7 DOF serial humanoid arm

3.1. Humanoid shoulder girdles

Despite the shoulder girdle's importance to human arm movements and workspace, few humanoid arms have a shoulder girdle. Kotaro is a humanoid robot that has a parallel shoulder girdle that replicates the physical shape and structure of the human scapular and clavicle [9]. Lenarčič et al present a parallel humanoid shoulder girdle structure in [10]. Parallel structured shoulder girdles have the advantage of being able to handle large loads, however, they have the disadvantage of having complex kinematics. Tondu presents a two DOF serial shoulder girdle in [11] which has the advantage of simplicity while still preforming the required shoulder girdle functions. WE-4RII is a humanoid robot with a two DOF serial shoulder girdle [12].

3.2. Humanoid glenohumeral joint singularity

Another limitation of typical humanoid arms arises because each DOF of the humanoid arm is assigned to a separate joint. Such splitting of a three DOF joint into three separate one DOF joints results in a kinematic singularity. That is, at certain arm postures, it is impossible to generate arm velocities in certain directions [13]. The singularity occurs at 90 degrees abduction when two DOFs, flexion/extension and inward/outward rotation, line up, thus one DOF is lost (See Figure 7).

3.3. Human motion imitation of 7 DOF humanoid arms

According to human motion imitation attempts that have been carried out in literature, human motion had to be restricted in order to fit the robot capabilities. The shoulder limitations and

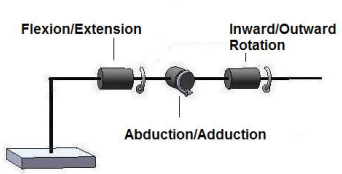

Figure 7: Singularity of the glenohumeral joint on serial humanoid arms - flexion/extension and inward/outward rotation line up thus one DOF is lost

the glenohumeral joint singularity also hampered the humanoid robot motion as compared to human motion.

Pollard et al used a humanoid robot, ART(DB), to perform the motions of the song 'I'm a little teapot' from motion capture of different actors. They found that the humanoid's limited shoulder motion, as well avoiding contact of the humanoid arm with the rest of the body, affected the humanoid's performance [14]. Riley et al used a Sarcos humanoid robot to perform a dance from human motion capture. The robot's trajectory differed from the human's due to the robot joint limits [15]. HRP-1S was used by Nakaoka et al to perform a captured traditional Japanese dance. They found that certain important postures of the dance were lost due to modifying the human trajectories to fit the humanoid robot structure [16]. Dariush et al used the humanoid ASIMO to imitate human motions from motion descriptors derived from visual motion capture. They found that the shape and limited DOFs of the humanoid were two of the factors that caused a discrepancy between the humanoid and human motions [17].

4. 10 DOF humanoid arm

The kinematics design for a ten DOF humanoid robot addresses the limitations of typical humanoid arms. The aim of the design is to make the robot fit for human motions rather than having to restrict human motions to fit the robot's limitations. Figure 8 shows the structure of the ten DOF humanoid arm.

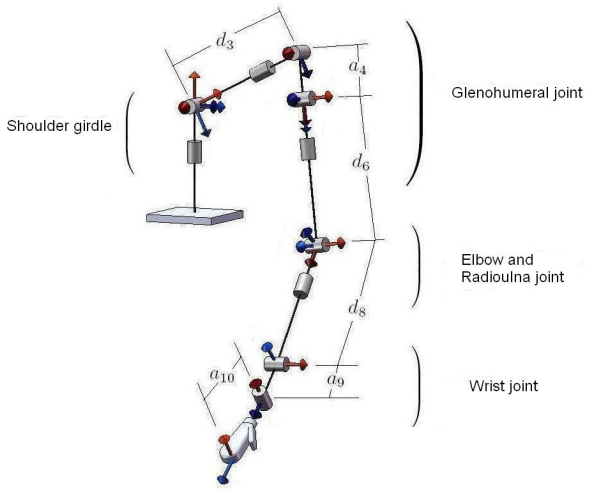

Figure 8: Kinematic structure and Denavit-Hartenberg parameters (Link length a and joint offset d) for a 10 DOF humanoid arm with a shoulder girdle and a 4 DOF glenohumeral joint

4.1. 2 DOF shoulder girdle

To address the lack of a humanoid shoulder girdle, a two DOF shoulder girdle structure, similar to that found in [12], is added to the conventional seven DOF arm. The two DOFs are protraction/retraction and a combination of elevation/depression and upward tilt. The two DOFs, elevation/depression and upward tilt, are combined because they perform similar functions when it comes to the arm movements; i.e. they both lift the centre of rotation of the glenohumeral joint.

4.2. 4 DOF glenohumeral joint

To address the singularity problem the glenohumeral joint is endowed with redundancy. Redundancy is defined as when the joint has more DOFs than those strictly required to execute a given task. This means that the same task can be executed in different ways at the individual DOFs and this can be exploited to avoid singularities [13]. Therefore a four DOF glenohumeral joint that can avoid the singularity found at three DOF joints while retaining the required robot motion is employed (See Figure 8).

5. Visual motion capture and transfer

The visual motion capture system which was used for motion transfer to the arm consists of 16 passive markers placed on the dancer and six independent digital video cameras capturing the dance routine at 50Hz. The African dance routine was performed inside a pre-calibrated area. The motion capture data was post-processed to manually identify the various markers. Each marker was plotted manually for each individual frame, for each camera. The current processing time for the motion capture data is six person hours per second of video footage. Figure 9 shows the location of the motion markers on the dancer.

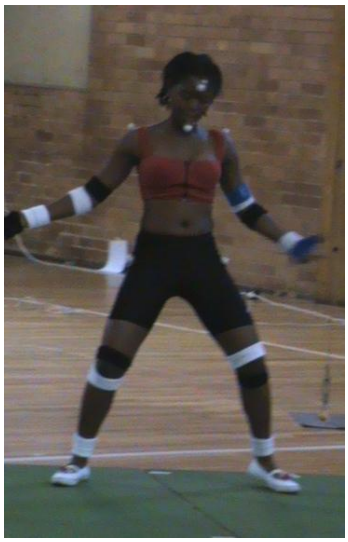

Figure 9: Human dancer with 16 motion capture markers located at: forehead, chin, glenohumeral joints, elbow joints, wrist joints, hips, knees, ankles and feet

5.1. Calculating humanoid joint angles for trajectory imitation

The available motion capture data from this visual motion capture system gives the position coordinates of the wrist, elbow and glenohumeral joints which in turn would give the various joint angles that enable the humanoid arm to follow the desired human trajectory. Given the reference frame for the arm movements and the initial posture of the arm, the joint angles can be calculated using [8] [13]:

$$\boldsymbol{q}(t_{k+1}) = \boldsymbol{q}(t_k) + \dot{\boldsymbol{q}}(t_k)\Delta t$$

where $\boldsymbol{q}$ is the vector of joint angles and Δt is a time interval.

Joint angular velocities can be obtained from the marker linear velocities $\boldsymbol{v}$ by inverting the Jacobian matrix $\boldsymbol{J}$. The damped least-squares Jacobian $\boldsymbol{J}^\star$, given by [8] [13], is used:

$$\boldsymbol{J}^\star = \boldsymbol{J}^T(\boldsymbol{J}\boldsymbol{J}^T + \lambda^2 I)^{-1}$$

where λ is a damping constant.

An objective function that keeps the joints away from singular positions is added giving [8] [13]:

$$\dot{\boldsymbol{q}} = \boldsymbol{J}^\star \boldsymbol{v} + (\boldsymbol{I} - \boldsymbol{J}^\star \boldsymbol{J})\dot{\boldsymbol{q}}_0$$

where

$$\dot{\boldsymbol{q}}_0 = k_0 \left(\frac{\partial w(\boldsymbol{q})}{\partial \boldsymbol{q}} \right)^T$$

$k_0 > 0$ and $w(\boldsymbol{q})$ is an objective function of the joint variables.

5.2. Motion reference frames from the motion capture data

For the seven DOF arm, the position and orientation of the glenohumeral joint is used as the reference frame for calculating the arm joint movements. The mid-hip point is used as the global reference frame. The position of the glenohumeral joint with respect to the mid-hip point is calculated from the motion capture data. The orientation of the glenohumeral joint is obtained from computing the three DOFs of the spine with respect to the mid-hip point. The three spine DOFs are computed using the following estimates for the spine and clavicle link lengths; L_g, the link length for the clavicles is the distance between the left and right glenohumeral markers, and L_{gs}, the spine link length is the distance from the midpoint between the left and right glenohumeral markers to the midpoint between the left and right hip markers.

For the ten DOF arm, the position and orientation of the sternum is used as the reference frame for calculating the shoulder girdle and arm joint movements. To obtain the shoulder girdle DOFs, markers on the chest and sternum would be required which give the sternum position and orientation with respect to the mid hip point. However, because of the post-processing required, adding more motion capture markers onto the dancer would make the motion capture process more time consuming and expensive.

6. Sternum reference frame

To avoid the added time and expense of increasing the number of motion capture markers on the dancer, a formulation that calculates the required sternum position and orientation without need of extra markers is used. The formulation uses the workspaces of the spine and the clavicles.

6.1. Sternum position formulation

The sternum is found at the intersection of the spine and the left and right clavicles. To find the intersection point, the spine can be taken as a link with length L_s centred at the mid-hip position. The clavicles can be taken as links with lengths L_c centred at the glenohumeral joints $\begin{pmatrix} a_L & b_L & c_L \end{pmatrix}$ and $\begin{pmatrix} a_R & b_R & c_R \end{pmatrix}$. (See Figure 10).

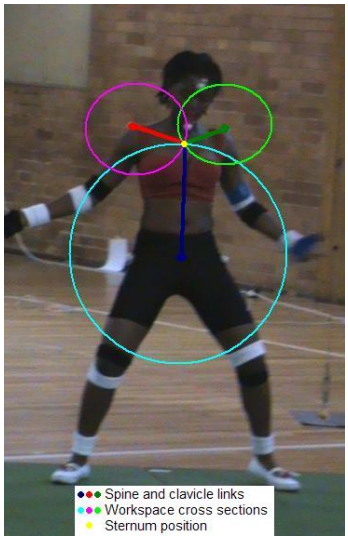

Figure 10: Dancer showing the spine and clavicle links, and their workspace cross-sections, centred at the glenohumeral markers and mid-hip point, to find the position of sternum

The workspace of each link is a sphere centred at the glenohumeral joints and mid-hip point respectively. The intersection of the three workspaces gives two possible sternum positions (See Figures 11 and 12). To choose between the two sternum positions, the one that keeps the sternum forwards in relation to the rest of the body is selected.

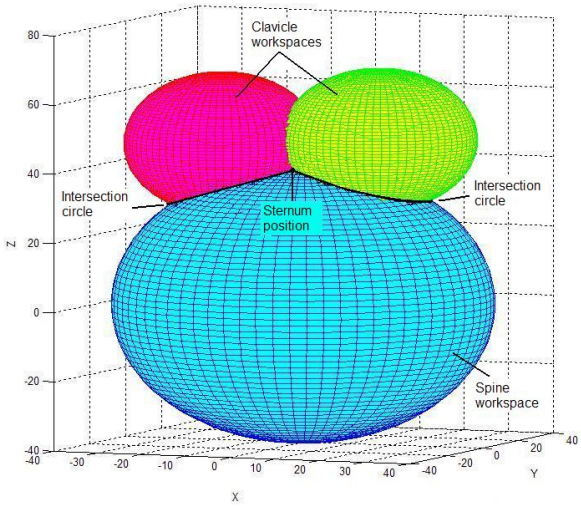

Figure 11: Spine and clavicles' spherical workspaces and intersection circles to find the sternum position

The equations of the spherical workspaces are given by (subscripts for the left clavicle, right clavicle and spine links are omitted):

$$L^2 = (x-a)^2 + (y-b)^2 + (z-c)^2$$

The intersection of the spine sphere with each clavicle sphere is a circle (See Figures 11 and 12). Combining the equations of the spheres gives the equations of the two planes on which the intersection circles of the spheres lie :

$$d_p = a_p x + b_p y + c_p z$$

The position of the centre $\boldsymbol{C}$ of each intersection circle is

$$\boldsymbol{C} = d_p \times \boldsymbol{n}_p$$

where $\boldsymbol{n}_p$ is the normal of the plane.

The radius r_I of each intersection circle is

$$r_I = \sqrt{L_s^2 - d_p^2}$$

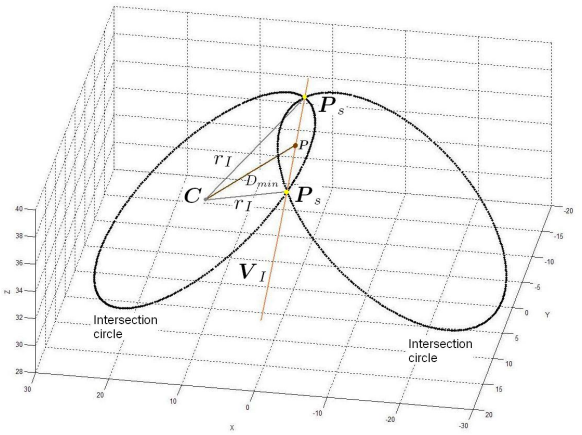

Figure 12: Intersection circles of the spine workspace with the two clavicle workspaces showing the two possible sternum points $\boldsymbol{P_s}$, the intersection circle centre $\boldsymbol{C}$, the intersection circle radius r_I, the line of intersection $\boldsymbol{V_I}$, the point P, and the minimum distance D_{min} between $\boldsymbol{V_I}$ and $\boldsymbol{C}$

Finding the intersection of the two intersection circles then gives the two possible sternum positions $\boldsymbol{P}_s$ as shown in Figure 12. To find the possible sternum positions, first we find the line of intersection $\boldsymbol{V}_I$ of the two intersection planes:

$$\boldsymbol{V}_I = \boldsymbol{n}_{pL} \times \boldsymbol{n}_{pR}$$

The intersection of one of the intersection circles with the line then gives the two possible sternum points:

$$\boldsymbol{P}_s = \boldsymbol{P} \pm D\boldsymbol{V}_I$$

where the point $\boldsymbol{P}$ is

$$\boldsymbol{P} = \boldsymbol{C} + D_{min}(\boldsymbol{V}_I \times \boldsymbol{n}_p)$$

and the distance D is:

$$D = \sqrt{r_I^2 - D_{min}^2}$$

where r_I is the radius of the intersection circle

and D_{min} is the minimum distance between the line of intersection and the centre $\boldsymbol{C}$ of the intersection circle.

6.2. Link length estimates

For the sternum position formulation, the link lengths of the spine and clavicles are estimated using the geometry of the body. The clavicle link lengths are equivalent to the distances between each glenohumeral marker and the sternum. From the body geometry, the distance between the two glenohumeral markers L_g is less than the combined clavicle link lengths. The link lengths L_c of the clavicles are therefore taken as:

$$L_c = \frac{1}{2}\left(L_g + \frac{A_g - M_g}{2}\right)$$

where A_g is the average female shoulder breath obtained from [18] and is equal to 395mm

and M_g is the average distance between the glenohumeral joints for all the motion capture frames.

The spine link length is the distance between the mid-hip point and the sternum. From the body geometry, the spine link length is less than the distance L_{gs} between the mid-hip and mid-glenohumeral joint points. The spine link length L_s is thus taken as:

$$L_s = L_{gs} - \frac{3(A_{gs} - M_{gs})}{2}$$

where A_{gs} is the average female shoulder height (from hip to shoulder) obtained from [18] and is equal to 555mm

and M_{gs} is the average distance between the mid-hip and mid-glenohumeral points for all the motion capture frames.

The link lengths above serve as the initial inputs into the sternum formulation. For any frame where the spine workspace does not intersect with the clavicle workspaces, the spine length is increased. Finally to obtain two distinct possible sternum positions, the spine link length and the clavicle link lengths are increased by a fraction of their lengths. The resulting link lengths are then used in a second iteration of the sternum position formulation to obtain the final sternum estimates.

6.3. Testing of sternum formulation

To test the formulation the calculated sternum position is compared with a test case (See Figure 13). A freely available motion data set that contains a sternum marker [19] is used as the test data set. The test data set does not contain a large variety of arm movements but is still sufficient to test and validate the sternum position formulation.

Figure 13 shows the xyz positions of the sternum marker and the calculated position of the sternum. The plots for the calculated and actual sternum positions are similar and so the presented sternum formulation can reliably be used.

7. Conclusions

This paper has presented the kinematics structure for a humanoid service robot arm. The humanoid arm structure has a two DOF shoulder girdle, a four DOF glenohumeral joint, a one DOF elbow joint, a one DOF radioulna joint and a two DOF wrist joint. This ten DOF arm structure addresses some of the limitations of conventional seven DOF humanoid robot arms and thus the ten DOF humanoid robot arm would be better suited than a seven DOF arm for use as a service or care robot within human environments.

The paper has also presented a method of calculating the sternum reference frame for the arm and shoulder girdle movements from human motion capture data. Testing of the sternum formulation method shows that the calculated sternum po-

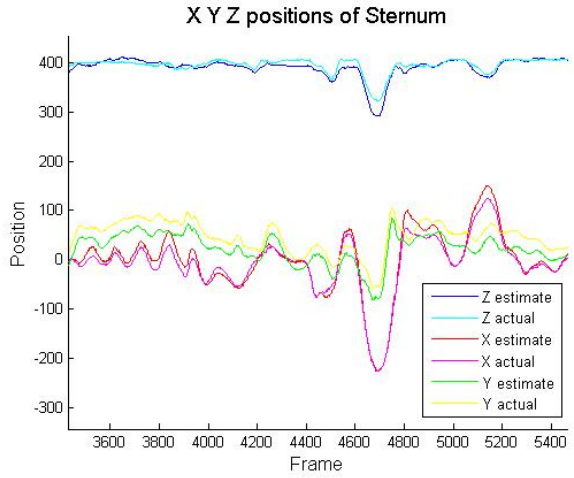

Figure 13: Actual and calculated sternum positions of a test motion capture data set

sition corresponds well to the actual sternum position of the human. The sternum formulation can therefore be used to produce a sternum reference frame for arm and shoulder girdle movements in place of an actual sternum motion capture marker.

Further studies include refining the link length estimates for the sternum position formulation, building a humanoid arm that has the proposed ten DOF structure and testing its motion imitation capabilities.

8. Acknowledgments

The research in this paper was funded by the Mobile Intelligent Autonomous Systems group (MIAS) of the Council for Scientific and Industrial Research (CSIR), South Africa. The African dance was choreographed by The Drum Cafe and the motion capture of the dance was carried out by the University of Johannesburg and the CSIR Sports Center. The authors would like to thank Ajith Gopal for his contributions to the African dance motion capture.

9. References

[1] Luttgens, K. and Wells, K. F., *Kinesiology : Scientific Basis of Human Motion*, 6th ed. Philadelphia: Saunders College Publishing, 1982.

[2] Hamill, J. and Knutzen, K. M., *Biomechanical Basis of Human Motion*, Baltimore: Williams and Wilkins, 1995.

[3] Lenarčič, J. and Klopčar, N.,"Positional kinematics of humanoid arms," *Robotica,* vol.24, pp. 105112, 2006.

[4] American Honda Motor Co. Inc. Corporate affairs & Communication, "Asimo the Honda humanoid robot," American Honda Motor Co. Inc., Technical Information, 2003.

[5] Kaneko, K., Kanehiro, F., Kajita, S., Hirukawa, H., Kawasaki, T., Hirata, M., Akachi, K. and Isozumi, T., "Humanoid robot HRP-2," *Proceedings of 2004 IEEE International Conference on Robotics and Automation,* New Orleans, LA, pp. 1083- 1090 vol.2, Apr 2004.

[6] Park, I., Kim, J., Lee J. and Oh J., "Mechanical design of humanoid robot platform KHR-3 (KAIST humanoid robot - 3: HUBO)," *5th IEEE-RAS International Conference on Humanoid Robots,* pp. 321-326, Dec. 2005.

[7] Albers, A., Brudniok, S., Ottnad, J., Sauter, C. and Sedchaicharn, K. "Upper Body of a new Humanoid Robot - the design of ARMAR III," *6th IEEE-RAS International Conference on Humanoid Robots,* Genova, pp. 308-313, Dec. 2006.

[8] Sciavicco, L., Siciliano, B., *Modelling and Control of Robot Manipulators,* London: Springer-Verlag, 2005.

[9] Sodeyama, Y., Yoshikai, T., Nishino, T., Mizuuchi, I. and Inaba, M., "The Designs and Motions of a Shoulder Structure with a Wide Range of Movement Using Bladebone-Collarbone Structures," *Proceedings of the 2007 IEEE/RSJ International Conference on Intelligent Robots and Systems,* San Diego, CA, pp. 3629-3634, Oct. 2007.

[10] Lenarčič, J. and Klopčar, N., "Kinematic design of a humanoid robotic shoulder complex," *Proceedings of 2000 IEEE International Conference on Computational Intelligent Robots and Automation,* San Francisco, CA, pp. 27-32, Apr. 2000.

[11] Tondu, B., "Modelling of the shoulder complex and applications to the design of upper extremities for humanoid robots," *Proceedings of 2005 5th IEEE-RAS International Conference on Humanoid Robots,* pp. 313-320, 2005.

[12] Miwa, H., Itoh, K., Ito, D., Takanobu, H., Takanishi, A., "Design and control of 9-DOFs emotion expression humanoid arm", *2004 IEEE International Conference on Robotics and Automation,* New Orleans, LA, pp. 128-133, Apr. 2004.

[13] Chiaverini, S., Oriolo, G., Walker, I., "Kinematically redundant manipulators," *Springer Handbook of Robotics,* Siciliano, B. and Khatib, O., Eds, Berlin Heidelberg: Springer-Verlag, 2008, pp. 245-268.

[14] Pollard, N.S., Hodgins,J.K., Riley, M.J., Atkeson, C.G., "Adapting Human Motion for the Control of a Humanoid Robot," *2002 International Conference on Robotics and Automation,* pp. 1390-1397 vol.2, 2002.

[15] Riley, M.,Ude, A., Atkeson C.G., "Methods for Motion Generation and Interaction with a Humanoid Robot: Case Studies of Dancing and Catching," Georgia Institute of Technology, GVU Technical Report, 2000.

[16] Nakaoka, S., Nakazawa, A., Yokoi, K., Himkawa, H., Ikeuchi, K., "Generating Whole Body Motions for a Biped Humanoid Robot from Captured Human Dances," *Proceedings of the 2003 IEEE International Conference on Robotics & Automation,* Taipei, Taiwan, pp. 3905-3910, Sept. 2003.

[17] Dariush, B., Gienger, M., Jian, B., Goerick, C., Fujimura, K., "Whole body humanoid control from human motion descriptors", *2008 IEEE International Conference on Robotics and Automation,* Pasadena, CA, pp. 2677-2684, May. 2008.

[18] Pheasant, S., *Bodyspace : Anthrometry, Ergonomics and Design*, London and Philadelphia: Taylor and Francis, 1986.

[19] Advanced Computing Center for the Arts and Design, The Ohio State University